
THE SKEW-NORMAL DISTRIBUTION IN SPC*

Authors: FERNANDA FIGUEIREDO
– CEAUL and Faculdade de Economia da Universidade do Porto,
Portugal (otilia@fep.up.pt)

M. IVETTE GOMES
– Universidade de Lisboa, FCUL, DEIO and CEAUL,
Portugal (ivette.gomes@fc.ul.pt)

Abstract:

- Modeling real data sets, even when we have some potential (as)symmetric models for the underlying data distribution, is always a very difficult task due to some uncontrollable perturbation factors. The analysis of different data sets from diverse areas of application, and in particular from Statistical Process Control (SPC), lead us to notice they usually exhibit moderate to strong asymmetry as well as light to heavy tails, which leads us to conclude that in most of the cases, fitting a normal distribution to the data is not the best option, despite of the simplicity and popularity of the Gaussian distribution. In this paper we consider a class of skew-normal models that include the normal distribution as a particular member. Some properties of the distributions belonging to this class are enhanced in order to motivate their use in applications. To monitor industrial processes some control charts for skew-normal and bivariate normal processes are developed, and their performance analysed. An application to a real data set from a cork stopper's process production is presented.

Key-Words:

- *Bootstrap control charts; Control charts; Heavy-tails; Monte Carlo simulations; Skewness; Skew-normal distribution; Statistical process control.*

AMS Subject Classification:

- 62E15, 62F40, 62F86, 62P30, 65C05.

*Research partially supported by National Funds through **FCT**—Fundação para a Ciência e a Tecnologia, project PEst-OE/MAT/UI0006/2011.

1. Introduction

The most commonly used standard procedures of Statistical Quality Control (SQC), control charts and acceptance sampling plans, are often implemented under the assumption of normal data, which rarely holds in practice. The analysis of several data sets from diverse areas of application, such as, statistical process control (SPC), reliability, telecommunications, environment, climatology and finance, among others, lead us to notice that this type of data usually exhibit moderate to strong asymmetry as well as light or heavy tails. Thus, despite of the simplicity and popularity of the Gaussian distribution, we conclude that in most of the cases, fitting a normal distribution to the data is not the best option. On another side, modeling real data sets, even when we have some potential (as)symmetric models for the underlying data distribution, is always a very difficult task due to some uncontrollable perturbation factors.

This paper focus on the parametric family of skew-normal distributions introduced by O'Hagan and Leonard (1976), and then investigated with more detail by Azzalini (1985, 1986, 2005), among others.

Definition 1.1. A random variable (rv) Y is said to have a location-scale skew-normal distribution, with location λ , scale δ and shape parameter α , being denoted $Y \sim SN(\lambda, \delta^2, \alpha)$, if its probability density function (pdf) is given by

$$(1.1) \quad f(y; \lambda, \delta, \alpha) = \frac{2}{\delta} \phi\left(\frac{y - \lambda}{\delta}\right) \Phi\left(\alpha \frac{y - \lambda}{\delta}\right), \quad y \in \mathbb{R} \quad (\alpha, \lambda \in \mathbb{R}, \delta \in \mathbb{R}^+),$$

where ϕ and Φ denote, as usual, the pdf and the cumulative distribution function (cdf) of the standard normal distribution, respectively. If $\lambda = 0$ and $\delta = 1$, we obtain the standard skew-normal distribution, denoted $SN(\alpha)$.

This class of distributions includes models with different levels of skewness and kurtosis, apart from the normal distribution itself ($\alpha = 0$). In this sense, it can be considered an extension of the normal family. Allowing departures from the normal model, by the introduction of the extra parameter α that controls the skewness, its use in applications will provide more robustness in inferential methods, and probably, better models to fit the data, for instance, when the empirical distribution has a shape similar to the normal, but exhibits asymmetry. Note that even in potential normal situations there is some possibility of having disturbances in the data, and the skew-normal family of distributions can describe the process data in a more reliable and robust way. In applications it is also important to have the possibility of regulating the thickness of the tails, apart of the skewness.

The cdf of the skew-normal rv Y defined in (1.1) is given by

$$(1.2) \quad F(y; \lambda, \delta, \alpha) = \Phi\left(\frac{y - \lambda}{\delta}\right) - 2T\left(\frac{y - \lambda}{\delta}, \alpha\right), \quad y \in \mathbb{R} \quad (\alpha, \lambda \in \mathbb{R}, \delta \in \mathbb{R}^+),$$

where $T(h, b)$ is the Owen's T function (integral of the standard normal bivariate density, bounded by $x = h$, $y = 0$ and $y = bx$), tabulated in Owen (1956).

Although the pdf in (1.1) has a very simple expression the same does not happen with the cdf in (1.2), but this is not a problem that lead us to avoid the use of the skew-normal distribution. The R package 'sn' (version 0.4-17), developed by Azzalini (2011), is now available. In such a package, functions related to the skew-normal distribution, like the density function, the distribution function, the quantile function, random number generation and maximum likelihood estimates are provided.

The moment generating function of the rv Y is given by

$$(1.3) \quad M_Y(t) = 2 \exp(\lambda t + \delta^2 t^2 / 2) \Phi(\theta \delta t), \quad \forall t \in \mathbb{R},$$

where $\theta = \alpha / \sqrt{1 + \alpha^2} \in (-1, 1)$, and there exist finite moments of all orders.

Other classes of skew normal distributions, for the univariate and the multivariate case, together with the related classes of skew-t distributions, have been recently revisited and studied in the literature. For details see Fernandez and Steel (1998), Abtahi *et al.* (2011) and Jamalizadeb *et al.* (2011), among others.

This paper is organised as follows. Section 2 provides some information about the family of skew-normal distributions considered in this study, in what concerns properties, random sample generation and inference. Section 3 presents some control charts based on the skew-normal distribution. Bootstrap control charts for skew-normal processes are developed and some simulation results about their performance are presented. Control charts based on specific statistics with skew normal distribution are considered to monitor bivariate normal processes, and their properties evaluated. In Section 4, an application in the field of SPC is provided.

2. The univariate skew-normal family of distributions

Without loss of generality, we are going to enhance some properties of this family of distributions by considering a standard skew-normal rv X , with pdf

$$(2.1) \quad f(x; \alpha) = 2\phi(x)\Phi(\alpha x), \quad x \in \mathbb{R} \quad (\alpha \in \mathbb{R}).$$

Note that, if $Y \sim SN(\lambda, \delta^2, \alpha)$ then $X = \frac{Y - \lambda}{\delta} \sim SN(\alpha)$.

2.1. An overview of some properties

In Figure 1 we illustrate the shape of the pdf of X for several values of α . We easily observe that the shape parameter α controls the direction and the magnitude of the skewness exhibited by the pdf. As $\alpha \rightarrow \pm\infty$ the asymmetry of the pdf increases, and if the sign of α changes, the pdf is reflected on the opposite side of the vertical axis. For $\alpha > 0$ the pdf exhibits positive asymmetry, and for $\alpha < 0$ the asymmetry is negative.

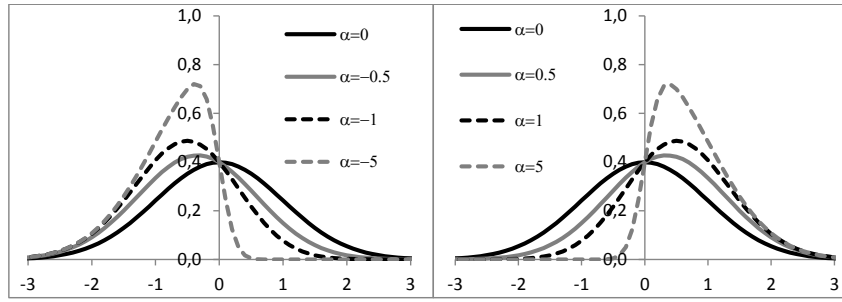


Figure 1: Density functions of standard skew-normal distributions with shape parameter α .

Proposition 2.1. As $\alpha \rightarrow \pm\infty$ the pdf of the rv X converges to a half-normal distribution. If $\alpha \rightarrow +\infty$, the pdf converges to $f(x) = 2\phi(x)$, $x \geq 0$, and if $\alpha \rightarrow -\infty$, the pdf converges to $f(x) = 2\phi(x)$, $x \leq 0$.

Proposition 2.2. If $X \sim SN(\alpha)$ then the rv $W = |X|$ has a half-normal distribution with pdf given by $f(w) = 2\phi(w)$, $w \geq 0$, and the rv $T = X^2$ has a pdf given by $f(t) = \frac{1}{\sqrt{2\pi}}t^{-1/2}e^{-t/2}$, $t \geq 0$, i.e., has a chi-square distribution with 1 degree of freedom.

Denoting the usual sign function by $sign(\cdot)$ and taking $\theta = \alpha/\sqrt{1+\alpha^2}$, the rv X with a standard skew-normal distribution $SN(\alpha)$ has a mean value given by

$$\mathbb{E}(X) = \sqrt{\frac{2}{\pi}} \theta \xrightarrow{\alpha \rightarrow \pm\infty} sign(\alpha) \times 0.79788,$$

variance equal to

$$\mathbb{V}(X) = 1 - \frac{2}{\pi} \theta^2 \xrightarrow{\alpha \rightarrow \pm\infty} 0.36338,$$

and the Fisher coefficient of skewness is given by

$$\beta_1 = \frac{(4 - \pi)\sqrt{2\theta^6/\pi^3}}{\sqrt{-8\theta^6/\pi^3 + 12\theta^4/\pi^2 - 6\theta^2/\pi + 1}} \xrightarrow{\alpha \rightarrow \pm\infty} \text{sign}(\alpha) \times 0.99527.$$

From these expressions we easily observe that the mean value and the degree of skewness of the $SN(\alpha)$ distribution increases with $|\alpha|$ while the variance decreases, but all of them converge to a finite value.

Taking into consideration the large asymmetry of the $SN(\alpha)$ distribution when $\alpha \rightarrow \pm\infty$, and the fact of the kurtosis coefficient express a balanced weight of the two-tails, we shall here evaluate separately the right-tail weight and the left-tail weight of the $SN(\alpha)$ distribution through the coefficients τ_R and τ_L defined by

$$\tau_R := \left(\frac{F^{-1}(0.99) - F^{-1}(0.5)}{F^{-1}(0.75) - F^{-1}(0.5)} \right) \left(\frac{\Phi^{-1}(0.99) - \Phi^{-1}(0.5)}{\Phi^{-1}(0.75) - \Phi^{-1}(0.5)} \right)^{-1}$$

and

$$\tau_L := \left(\frac{F^{-1}(0.5) - F^{-1}(0.01)}{F^{-1}(0.5) - F^{-1}(0.25)} \right) \left(\frac{\Phi^{-1}(0.5) - \Phi^{-1}(0.01)}{\Phi^{-1}(0.5) - \Phi^{-1}(0.25)} \right)^{-1},$$

where F^{-1} and Φ^{-1} denote the inverse functions of the cdf of the $SN(\alpha)$ and of the cdf of the standard normal distributions, respectively. These coefficients are based on the tail-weight coefficient τ defined in Hoaglin *et al.* (1983) for symmetric distributions. For the normal distribution, $\tau_L = \tau_R = 1$. If the distribution F has a right (left) tail heavier than the normal tails, $\tau_R > 1$ ($\tau_L > 1$), and if F has a right (left) tail thinner than the normal tails, $\tau_R < 1$ ($\tau_L < 1$).

Table 1 presents the mean value, the standard deviation, the median, the skewness coefficient, the left-tail weight and the right-tail weight of the $SN(\alpha)$ distribution for several values of $\alpha > 0$. From the values of Table 1 we notice that when α increases from 0 to $+\infty$, the mean value, the median and the coefficient of skewness increases, but the variance decreases, as expected. The $SN(\alpha)$ distribution has a right-tail heavier than the normal tail, and a left-tail thinner than the normal tail. Moreover, the right tail-weight of the $SN(\alpha)$ quickly converges to 1.1585, the right tail-weight of the half-normal distribution, while the left tail-weight of the $SN(\alpha)$ converges more slowly to the left tail-weight of the half-normal distribution, 0.5393, a value very smaller than the tail-weight of the normal distribution. When α decreases from 0 to $-\infty$ we easily obtain the values of these parameters (coefficients) from the values of this table, taking into consideration that if the sign of α changes, the pdf is reflected on the opposite side of the vertical axis.

Table 1: Mean value (μ), standard deviation (σ), median (μ_e), skewness coefficient (β_1), left-tail weight (τ_L) and right-tail weight (τ_R) of the $SN(\alpha)$ distribution.

α	μ	σ	μ_e	β_1	τ_L	τ_R
0	0	1	0	0	1	1
0.3	0.2293	0.9734	0.2284	0.0056	0.9986	1.0017
0.5	0.3568	0.9342	0.3531	0.0239	0.9946	1.0077
1	0.5642	0.8256	0.5450	0.1369	0.9718	1.0457
2	0.7136	0.7005	0.6554	0.4538	0.9008	1.1284
3	0.7569	0.6535	0.6720	0.6670	0.8291	1.1540
5	0.7824	0.6228	0.6748	0.8510	0.7222	1.1584
10	0.7939	0.6080	0.6745	0.9556	0.6124	1.1585
$+\infty$	0.7979	0.6028	0.6745	0.9953	0.5393	1.1585

2.2. Inference

Regarding parameters' estimation in the location-scale skew-normal family of distributions, $SN(\lambda, \delta^2, \alpha)$, we are only able to obtain numerical maximum likelihood estimates (MLEs), and thus, a closed form for their sampling distribution is not available.

Let (Y_1, \dots, Y_n) be a sample of size n from a $SN(\lambda, \delta^2, \alpha)$ distribution. The likelihood function is given by

$$(2.2) \quad L_{SN}(\lambda, \delta, \alpha) = \frac{2^n}{\delta^n} \prod_{i=1}^n \phi\left(\frac{y_i - \lambda}{\delta}\right) \prod_{i=1}^n \Phi\left(\alpha \frac{y_i - \lambda}{\delta}\right)$$

and the log-likelihood is given by

$$(2.3) \quad \ln L_{SN}(\lambda, \delta, \alpha) = n \ln 2 - n \ln \delta + \sum_{i=1}^n \ln \phi\left(\frac{y_i - \lambda}{\delta}\right) + \sum_{i=1}^n \ln \Phi\left(\alpha \frac{y_i - \lambda}{\delta}\right)$$

where $\ln(\cdot)$ denotes the natural logarithm function.

The MLE of λ , δ and α , denoted $\hat{\lambda}$, $\hat{\delta}$ and $\hat{\alpha}$, are the numerical solution of the system of equations

$$(2.4) \quad \begin{cases} \delta^2 = \frac{1}{n} \sum_{i=1}^n (y_i - \lambda)^2 \\ \alpha \sum_{i=1}^n \frac{\phi\left(\alpha \frac{y_i - \lambda}{\delta}\right)}{\Phi\left(\alpha \frac{y_i - \lambda}{\delta}\right)} = \sum_{i=1}^n \frac{y_i - \lambda}{\delta} \\ \sum_{i=1}^n \frac{\frac{y_i - \lambda}{\delta} \phi\left(\alpha \frac{y_i - \lambda}{\delta}\right)}{\Phi\left(\alpha \frac{y_i - \lambda}{\delta}\right)} = 0. \end{cases}$$

We may have some problems to obtain these estimates in the case of small-to-moderate values of the sample size n as well as for values of α close to zero. Note that if all the values of the sample are positive (negative), for fixed values of λ and δ , the log-likelihood function is an increasing (decreasing) function of α , producing therefore boundary estimates, and for $\alpha = 0$, the expected Fisher information matrix is singular.

Several authors have given important suggestions to find these estimates. For instance, for a fixed value of α , solve the last two equations of (2.4) for obtaining λ and δ , taking into account the first equation, and then, repeat these steps for a reasonable range of values of α . Another suggestion to get around these problems of estimation is to consider another re-parametrization for the skew-normal distributions $SN(\lambda, \delta^2, \alpha)$ in (1.1), in terms of the mean value μ , the standard deviation σ and the asymmetry coefficient β_1 . For details on this topic see, for instance, Azzalini (1985) and Azzalini and Capitanio (1999), among others.

To decide between the use of a normal or a skew-normal distribution to fit the available data, apart from the information given by the histogram associated to the data sample and the fitted pdf estimated by maximum likelihood, we can advance to the confirmatory phase with a likelihood ratio test.

To test the normal distribution against a skew-normal distribution, i.e., to test the hypotheses $H_0 : X \sim SN(\lambda, \delta^2, \alpha = 0)$ versus $H_1 : X \sim SN(\lambda, \delta^2, \alpha \neq 0)$, the likelihood ratio statistic Λ is given by

$$(2.5) \quad \Lambda = \frac{L_{SN}(\hat{\lambda}, \hat{\delta}, \alpha = 0)}{L_{SN}(\hat{\lambda}, \hat{\delta}, \hat{\alpha})},$$

where $L_{SN}(\lambda, \delta, \alpha)$ denotes the likelihood function for the $SN(\lambda, \delta^2, \alpha)$ distribution. Under the null hypothesis, $-2 \log \Lambda$ is distributed as a chi-square distribution with 1 degree of freedom. For a large observed value of $-2 \log \Lambda$, we reject the null hypothesis, i.e., there is a strong evidence that the $SN(\hat{\lambda}, \hat{\delta}^2, \hat{\alpha})$ distribution presents a better fit to the data set under consideration than the normal $N(\hat{\mu}, \hat{\sigma}^2)$ distribution.

2.3. Other stochastic results

Among other results valid for the skew-normal distribution, we shall refer the following ones:

Proposition 2.3. *If Z_1 and Z_2 are independent rvs with standard normal distribution, then $Z_1|_{Z_2 \leq \alpha Z_1} \sim SN(\alpha)$.*

Proposition 2.3 allow us to write the following algorithm for the generation of random samples, (Y_1, \dots, Y_n) , of size n , from a $SN(\lambda, \delta^2, \alpha)$ distribution.

Algorithm 2.1. Repeat steps 1.-4. for $i = 1$ to n :

1. Generate two independent values, Z_1 and Z_2 , from a $N(0, 1)$ distribution;
2. Compute $T = \alpha Z_2$;
3. The value $X_i = \begin{cases} Z_2, & \text{if } Z_1 < T \\ -Z_2, & \text{otherwise} \end{cases}$ comes from a $SN(\alpha)$;
4. The value $Y_i = \lambda + \delta X_i$ comes from a $SN(\lambda, \delta^2, \alpha)$.

Figure 2 presents four histograms associated to samples of size one thousand generated from a $SN(\alpha)$ distribution with shape parameter $\alpha = 0, 1, 2, 3$, respectively, together with the pdf's of a normal and of a skew normal distribution fitted to the data by maximum likelihood. From Figure 2 we easily observe that as α increases the differences between the two estimated pdfs become larger, and the normal fit is not the most appropriate to describe the data. Note that, even in potential normal processes, real data are not exactly normal and usually exhibit some level of asymmetry. Thus, in practice, we advise the use of the skew-normal distribution to model the data.

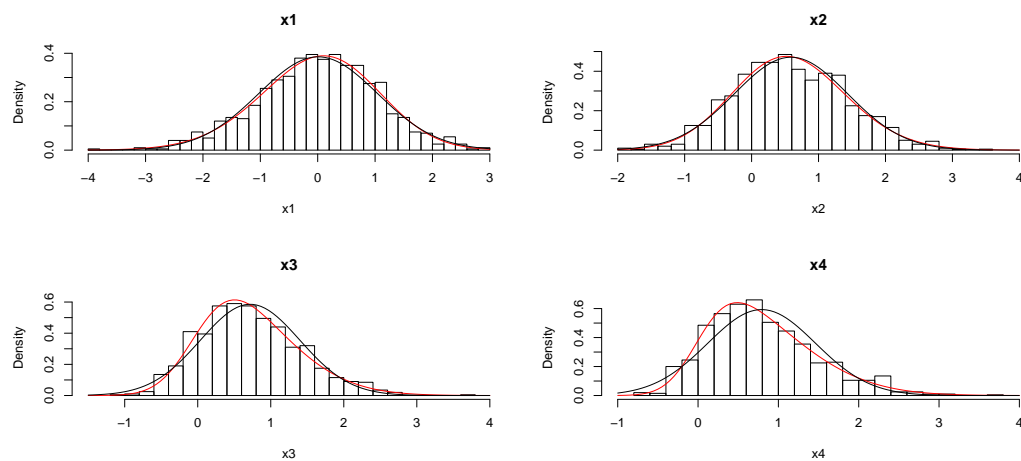


Figure 2: $X_1 \sim SN(0)$, $X_2 \sim SN(1)$, $X_3 \sim SN(2)$, $X_4 \sim SN(3)$. Histograms and estimated pdf, $SN(\hat{\lambda}, \hat{\delta}, \hat{\alpha})$ and $N(\hat{\mu}, \hat{\sigma})$.

Another result with high relevance for applications is the one presented in Proposition 2.4.

Proposition 2.4. Let (Z_1, Z_2) be a bivariate normal variable, $E(Z_1) = E(Z_2) = 0$, $V(Z_1) = V(Z_2) = 1$ and $\text{corr}(Z_1, Z_2) = \rho$. Let $T_m = \min(Z_1, Z_2)$ and $T_M = \max(Z_1, Z_2)$, where $\min(\cdot)$ and $\max(\cdot)$ denote the minimum and the maximum operators, respectively.

- i. If $\rho = 1$, T_m and T_M have a $N(0, 1)$ distribution.
- ii. If $\rho = -1$, T_m and T_M have half-normal distributions, being $T_m \leq 0, \forall m$ and $T_M \geq 0, \forall M$.
- iii. If $|\rho| \neq 1$, $T_m \sim SN(-\alpha)$ and $T_M \sim SN(\alpha)$, with $\alpha = \sqrt{\frac{1-\rho}{1+\rho}}$.
In particular, if Z_1 and Z_2 are independent variables, $\rho = 0$, and then, $T_m \sim SN(-1)$ and $T_M \sim SN(1)$.

3. Control charts based on the skew-normal distribution

The most commonly used charts for monitoring industrial processes, or more precisely, a quality characteristic X at the targets μ_0 and σ_0 , the desired mean value and standard deviation of X , respectively, are the Shewhart control charts with 3-sigma control limits. More precisely, the sample mean chart (M -chart), the sample standard deviation chart (S -chart) and the sample range chart (R -chart), and are usually developed under the assumptions of independent and normally distributed data. Additionally, the target values μ_0 and σ_0 are not usually fixed given values, and we have to estimate them, in order to determine the control limits of the chart.

The ability of a control chart to detect process changes is usually measured by the expected number of samples taken before the chart signals, i.e., by its ARL (Average Run Length), together with the standard deviation of the Run Length distribution, SDRL.

Whenever implementing a control chart, a practical advice is that 3-sigma control limits should be avoided whenever the distribution of the control statistic is very asymmetric. In such a case, it is preferable to fix the control limits of the chart at adequate probability quantiles of the control statistic distribution, in order to obtain a fixed ARL when the process is in-control, usually 200, 370.4, 500 or 1000, or equivalently, the desired false alarm rate (FAR), i.e., the probability that an observation is considered as out-of-control when the process is actually in-control), usually 0.005, 0.0027, 0.002 or 0.001. General details about Shewhart control charts can be found, for instance, in Montgomery (2005).

In the case of skew-normal processes we do not have explicit formulas for the ML estimators of the location, scale and shape parameters, and thus, a closed-form for their sampling distribution is not available. The same happens for other statistics of interest, such as, the sample mean, the sample standard deviation, the sample range and the sample percentiles, among others. Thus, to monitor skew-normal processes, the bootstrap control charts are very useful, although with the disadvantage of a highly time-consuming Phase I. Moreover, many papers, see for instance, Sepala *et al.* (1996), Liu and Tang (1996) and Jones and

Woodall (1998), refer that for skewed distributions, bootstrap control charts have on average a better performance than the Shewhart control charts. Other details about the bootstrap methodology and bootstrap control charts can be found, for instance, in Efron and Tibshirani (1993), Bai and Choi (1995), Nichols and Padgett (2006) and Lio and Park (2008, 2010).

3.1. Bootstrap control charts for skew-normal processes

To construct a bootstrap control chart we only use the sample data to estimate the sampling distribution of the parameter estimator, and then, to determine appropriate control limits. Thus, only the usual assumptions of Phase II of SPC are required: process stable and independent and identically distributed subgroup observations. The following Algorithm 3.1., similar to the ones proposed in Nichols and Padgett (2006) and Lio and Park (2008, 2010), can be used to implement bootstrap control charts for subgroup samples of size n , that enable us to monitor the process mean value and the process standard deviation of a skew-normal distribution. This algorithm can be easily modified in order to implement bootstrap control charts for monitoring other parameters of interest.

Algorithm 3.1.

Phase I: Estimation and determination of the control limits

1. From an in-control and stable process, observe k , say 25 or 30, random samples of size n , assuming that the observations are independent and come from a skew-normal distribution, $SN(\lambda, \delta^2, \alpha)$.
2. Compute the MLEs of λ , δ and α , using the pooled sample of size $k \times n$.
3. Generate a parametric bootstrap sample of size n , (x_1^*, \dots, x_n^*) , from a skew-normal distribution, using the MLEs obtained in Step 2. as the distribution parameters.
4. Select the step associated to the chart you want to implement:
 - i. **Two-sided bootstrap M -chart** to monitor the process mean value μ : from the bootstrap subgroup sample obtained in Step 3., determine the sample mean, $\hat{\mu}^* = \bar{x}^*$.
 - ii. **Upper one-sided bootstrap S -chart** to monitor the process standard deviation σ : from the bootstrap subgroup sample obtained in Step 3., determine the sample standard deviation, $\hat{\sigma}^* = s^*$.
5. Repeat Steps 3-4, a large number of times, say $B = 10000$ times, obtaining B bootstrap estimates of the parameter of interest, in our case, the process mean value or the standard deviation.

6. Let γ , the desired FAR of the chart. Using the B bootstrap estimates obtained in Step 5.,
 - i. Find the $100(\gamma/2)$ th and $100(1-\gamma/2)$ th quantiles of the distribution of $\hat{\mu}^*$, i.e., the lower control limit LCL and the upper control limit UCL for the bootstrap M -chart of FAR= γ , respectively.
 - ii. Find the $100(1-\gamma)$ th quantile of the distribution of $\hat{\sigma}^*$, i.e., the upper control limit UCL for the bootstrap S -chart of FAR= γ . The lower control limit LCL is placed at 0.

Phase II: Process monitoring

7. Take subgroup samples of size n from the process at regular time intervals. For each subgroup, compute the estimate \bar{x} and s .
8. **Decision:**
 - i. If \bar{x} falls between LCL and UCL, the process is assumed to be in-control (targeting the nominal mean value); otherwise, i.e., if the estimate falls below the LCL or above the UCL, the chart signals that the process may be out-of-control.
 - ii. If s falls below the UCL, the process is assumed to be in-control (targeting the nominal standard deviation); otherwise, the chart signals that the process may be out-of-control.

In order to get information about the robustness of the bootstrap control limits, we must repeat the steps 1.-6. of Algorithm 3.1. a large number of times, say $r = 1000$, and then, compute the average of the obtained control limits, UCL and LCL, and their associated standard deviations. The simulations must be carried out with different subgroup sample sizes, n , and different levels of FAR, γ . From this simulation study one would expect that, when the subgroup sample size n increases, the control limits get closer together, and when FAR decreases, the limits become farther apart.

In this study, using Algorithm 3.1., we implemented M and S bootstrap control charts for subgroups of size $n = 5$, to monitor the process mean value of a skew-normal process at a target μ_0 , and the process standard deviation at a target σ_0 . Without loss of generality we assumed $\mu_0 = 0$, $\sigma_0 = 1$ and $\alpha = 0$. The main interest is to detect increases or decreases in μ and to detect increases in σ (and not decreases in σ). The FAR of the charts is equal to $\gamma = 0.0027$, which corresponds to an in-control average run length (ARL) of approximately 370.4. In Phase I we considered $k = 25$ subgroups of size $n = 5$.

The performance of these bootstrap control charts to detect changes in the process parameters is evaluated in terms of the ARL, for a few different magnitude changes. When the process changes from the in-control state to an out-of-control state we assume that $\mu = \mu_0 \rightarrow \mu_1 = \mu_0 + \delta\sigma_0$, $\delta \neq 0$ and/or

$\sigma = \sigma_0 \rightarrow \sigma_1 = \theta\sigma_0$, $\theta > 0$. In this paper we repeated steps 1.-6. of Algorithm 3.1. 30 times, and then, we have chosen a pair of control limits that allow us to obtain an in-control ARL approximately equal to 370.4, discarding the most extreme upper and lower control limits. Our goal, although out of the scope of this paper, is to improve this algorithm in order to obtain more accurate control limits without replication.

Table 2 presents the ARL values of the bootstrap M -chart and S -chart, and the associated standard deviation SDRL. Indeed, as can be seen from Table 2, the bootstrap control charts present an interesting performance, even when we consider small changes. As the magnitude of the change increases, the ARL values decrease quickly. Despite of the fact that, in SPC, the classical M and S control charts are much more popular, these charts are good competitors, even for the case of normal data if we have to estimate the target process values.

Table 2: ARL and SDRL of the bootstrap M and S charts for subgroups of size $n = 5$. In-control, $\mu_0 = 0$ and $\sigma_0 = 1$; when the process is out-of-control we assume or $\mu \rightarrow \mu_1 = \delta$ or $\sigma \rightarrow \sigma_1 = \theta$.

M-chart ($\mu \rightarrow \mu_1$)			S-chart ($\sigma \rightarrow \sigma_1$)		
δ	ARL	SDRL	θ	ARL	SDRL
0.0	370.5	(371.8)	1.0	370.6	(369.6)
0.1	371.7	(377.2)	1.1	322.7	(320.8)
0.3	168.3	(169.7)	1.2	109.7	(108.2)
0.5	61.5	(61.2)	1.3	48.4	(48.0)
1.0	8.4	(7.8)	1.4	25.4	(24.4)
1.5	2.4	(1.8)	1.5	15.1	(14.5)
2.0	1.3	(0.6)	1.6	10.0	(9.5)
2.5	1.0	(0.2)	1.7	7.2	(6.8)
-0.1	261.9	(261.4)	1.8	5.3	(4.8)
-0.3	90.7	(89.9)	1.9	4.2	(3.7)
-0.5	33.4	(32.4)	2.0	3.5	(2.9)
-1.0	5.0	(4.6)	2.5	1.9	(1.3)
-1.5	1.8	(1.2)			
-2.0	1.1	(0.4)			
-2.5	1.0	(0.1)			

3.2. Control charts for bivariate normal processes

Let (X_1, X_2) be a bivariate normal process and, without loss of generality, assume that the quality characteristics X_1 and X_2 are standard normal variables, possibly correlated, denoting ρ the correlation coefficient. The result presented in Proposition 2.4, allows us to design control charts based on the statistics $T_m = \min(X_1, X_2)$ and $T_M = \max(X_1, X_2)$ to monitor this bivariate normal process.

These univariate statistics enable the implementation of control charts, here denoted T_m -chart and T_M -chart, to monitor simultaneously two related quality characteristics, alternatives to the multivariate control charts based on the Hotelling (1947) statistic and its variants.

Moreover, these charts can be used when in each time of sampling we only have available one observation from each variable of interest, X_1 and X_2 , but can be extended to other situations. For instance, when the distributions of X_1 and X_2 have different parameters, replacing X_1 and X_2 by standardized data, and also when we have samples of size greater than one from each of the variables X_1 and X_2 , replacing the observations of the samples by the standardized sample means.

First we have implemented a two-sided T_M chart to detect changes in μ , from $\mu_0 = 0$ to $\mu_1 = \delta$, $\delta \neq 0$, assuming the standard deviation maintains at $\sigma_0 = 1$. We considered different magnitude changes, and apart from independent data we also considered correlated data with different levels of positive and negative correlation. The obtained ARL values are presented in Table 3.

Table 3: ARL of the two-sided T_M -chart, for $X_i \sim N(\mu, \sigma)$, $i = 1, 2$, $\text{corr}(X_1, X_2) = \rho$. In-control: $\mu = 0$, $\sigma = 1$; When the process is out-of-control, we assume that only $\mu \rightarrow \mu_1 = \delta \neq 0$.

$\mu_1 = \delta/\rho$	0	0.1	0.25	0.5	0.9	1	-0.25	-0.5
0.0	370.4	370.4	370.4	370.4	370.4	370.4	370.4	370.4
0.1	361.6	359.5	357.1	354.2	352.7	352.9	368.4	379.6
0.3	249.7	248.6	247.4	247.0	251.0	253.1	253.5	258.7
0.5	144.1	144.0	144.4	145.9	152.5	155.2	144.7	145.5
1.0	36.7	36.9	37.3	38.6	42.5	43.9	36.5	36.4
1.5	11.6	11.7	12.0	12.7	14.4	15.0	11.4	11.3
2.0	4.6	4.7	4.9	5.2	6.0	6.3	4.5	4.4
2.5	2.4	2.4	2.5	2.7	3.1	3.2	2.2	2.2
-0.1	330.8	334.7	339.6	345.9	352.1	352.9	318.2	298.2
-0.3	196.1	204.6	215.9	231.6	249.9	253.1	170.6	135.9
-0.5	100.8	107.9	117.9	132.6	151.5	155.2	80.6	56.8
-1.0	21.7	24.1	27.7	33.5	42.0	43.9	15.7	9.7
-1.5	6.7	7.5	8.8	10.9	14.2	15.0	4.8	3.1
-2.0	2.9	3.2	3.7	4.6	6.0	6.3	2.2	1.7
-2.5	1.7	1.9	2.1	2.4	3.1	3.2	1.4	1.2

From these values we observe that as the magnitude changes increases, the ARL decreases, as expected, and that reductions in μ are detected faster than increases. We easily observe that the level of correlation ρ does not have a great impact on the performance of the chart. However, if the quality characteristics, X_1 and X_2 , are positively correlated, the ARL's become larger as the level of correlation increases, i.e., the chart becomes less efficient to detect the change. On the other hand, the best performance of the chart is obtained when there is a decrease in the process mean value and the quality characteristics are negatively correlated. This control chart is not unbiased, and maybe due to this fact that we

have observed that this chart is not appropriate to detect simultaneous changes in μ and σ . Then, we have implemented an upper one-sided T_M -chart to detect changes in μ and/or σ .

Table 4: ARL of the upper one-sided T_M -chart, for $X_i \sim N(\mu, \sigma)$, $i = 1, 2$, $\text{corr}(X_1, X_2) = \rho$. In-control: $\mu = 0$, $\sigma = 1$; When the process is out-of-control, $\mu \rightarrow \mu_1 > 0$ and/or $\sigma \rightarrow \sigma_1 > 1$.

μ_1	σ_1 / ρ	0.0	0.1	0.25	0.5	0.9	1.0	-0.25	-0.5
0.0	1.0	370.4	370.4	370.4	370.4	370.4	370.4	370.4	370.4
	1.1	156.7	156.9	157.4	159.3	167.1	175.0	156.6	156.6
	1.5	22.2	22.4	22.8	23.8	27.6	31.4	22.0	22.0
	2.0	7.7	7.9	8.1	8.6	10.4	12.2	7.6	7.5
	2.5	4.6	4.7	4.9	5.2	6.4	7.5	4.5	4.4
0.1	1.0	268.0	268.1	268.4	269.3	272.3	273.4	268.0	268.0
	1.1	119.5	119.7	120.2	122.2	129.2	135.5	119.3	119.3
	1.5	19.0	19.2	19.5	20.5	23.8	27.1	18.8	18.8
	2.0	7.1	7.2	7.4	7.9	9.5	11.1	6.9	6.8
	2.5	4.3	4.4	4.6	4.9	6.0	7.1	4.2	4.1
0.3	1.0	144.4	144.5	145.0	146.6	151.4	153.1	144.2	144.2
	1.1	71.1	71.3	71.8	73.4	79.0	83.2	70.9	70.9
	1.5	14.2	14.3	14.6	15.4	18.0	20.4	14.0	13.9
	2.0	5.9	6.0	6.2	6.6	8.0	9.3	5.7	5.7
	2.5	3.8	3.9	4.1	4.4	5.3	6.2	3.7	3.6
0.5	1.0	80.7	80.9	81.4	82.9	87.4	89.0	80.0	80.5
	1.1	43.6	43.8	44.3	45.6	49.8	52.6	43.4	43.4
	1.5	10.7	10.8	11.1	11.7	13.8	15.6	10.5	10.5
	2.0	5.0	5.1	5.3	5.6	6.8	7.9	4.8	4.8
	2.5	3.4	3.5	3.6	3.9	4.7	5.5	3.3	3.2
1.0	1.0	22.2	22.4	22.7	23.6	26.0	26.8	22.0	22.0
	1.1	14.7	14.9	15.2	15.9	17.9	19.0	14.5	14.5
	1.5	5.7	5.8	6.0	6.4	7.6	8.5	5.6	5.5
	2.0	3.4	3.5	3.6	3.9	4.7	5.4	3.3	3.2
	2.5	2.6	2.7	2.8	3.0	3.6	4.2	2.5	2.4
1.5	1.0	7.7	7.8	8.1	8.5	9.6	10.0	7.6	7.5
	1.1	6.1	6.1	6.3	6.7	7.7	8.2	5.9	5.8
	1.5	3.4	3.5	3.6	3.9	4.6	5.1	3.3	3.2
	2.0	2.5	2.5	2.6	2.9	3.4	3.8	2.4	2.3
	2.5	2.1	2.2	2.2	2.4	2.9	3.3	2.0	1.9
2.0	1.0	3.4	3.5	3.6	3.9	4.4	4.6	3.3	3.2
	1.1	3.0	3.1	3.2	3.4	4.0	4.2	2.9	2.8
	1.5	2.3	2.3	2.4	2.6	3.0	3.3	2.1	2.1
	2.0	1.9	2.0	2.1	2.2	2.6	2.9	1.8	1.7
	2.5	1.8	1.8	1.9	2.0	2.4	2.7	1.7	1.6
2.5	1.0	1.9	2.0	2.0	2.2	2.5	2.6	1.8	1.7
	1.1	1.8	1.9	2.0	2.1	2.4	2.5	1.7	1.6
	1.5	1.7	1.7	1.8	1.9	2.2	2.4	1.6	1.5
	2.0	1.6	1.6	1.7	1.8	2.1	2.3	1.5	1.4
	2.5	1.5	1.5	1.6	1.7	2.0	2.2	1.4	1.3

From the ARL values presented in Table 4, we conclude that the upper one-sided T_M -chart presents an interesting performance to detect increases in one of the process' parameters, μ or σ , but also to detect simultaneous changes in these parameters. We observe again that the level of correlation, ρ , between the quality characteristics X_1 and X_2 , has a small impact on the performance of the chart. Finally, the lower one-sided T_m -chart will have a similar performance to detect changes from $\mu \rightarrow \mu_1 < 0$ and/or $\sigma \rightarrow \sigma_1 > 1$.

4. An application in the field of SPC

In this section we consider an application to real data from a cork stopper's process production. The objective is modeling and monitoring the data from this process. We thus know that the corks must have the following characteristics:

Table 5: Technical specifications: cork stoppers caliber 45mm×24mm.

Physical quality characteristic (mm)	Mean target	Tolerance interval
Length	45	45 ± 1
Diameter	24	24 ± 0.5

For this purpose we have collected from the process production a sample, of size $n = 1000$, of corks' lengths and diameters. First, we have fitted a normal and a skew-normal distribution to the data set. Looking to the histograms obtained from the sample data, presented in Figure 3, we see that both fits seem to be adequate, and that the differences between the two pdf's are small.

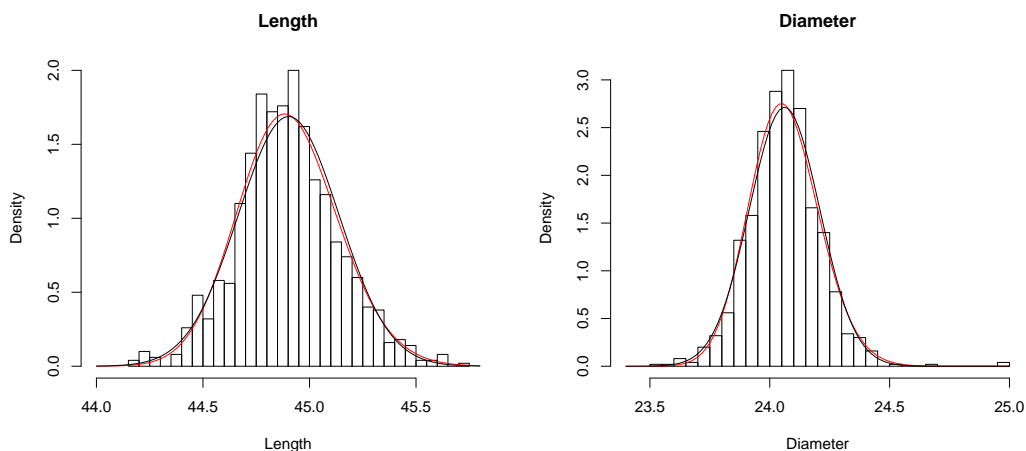


Figure 3: Histograms and estimated pdf's of the normal and skew-normal fit to the length and diameter data.

Then, to test the underlying data distribution, we have used the Shapiro test of normality and the Kolmogorov-Smirnov (K-S) for testing the skew-normal distribution. Unexpectedly, although the fits seem to be similar, from these tests of goodness-of-fit the conclusions are different: the normality for the length's and diameter's data is rejected, for the usual levels of significance (5% and 1%), while the skew-normal distribution is not rejected. The p -values for the Shapiro and K-S tests are presented in Table 6. Looking to the maximum likelihood estimates of some parameters of interest of the fitted distributions, presented in Table 7, we observe that there exist some differences between the estimates obtained for the mean value and the location, as well as between the estimates obtained for the standard deviation and the scale. Moreover, the data exhibit some skewness and the estimate of the shape parameter is not very close to zero, as it should happen in the case of normal data.

Table 6: P-value's of the Shapiro test of normality and of the Kolmogorov-Smirnov (K-S) for testing a skew-normal.

	Length	Diameter	Decision
Shapiro	0.00175	0.00515	Normality rejected*
K-S	0.2376	0.2923	The skew-normal distribution is not rejected*

*conclusion for a level of significance of 5% and 1%

Table 7: Maximum likelihood estimates of some parameters of interest of the fitted distributions, on the basis of a skew-normal model.

Data	Location	Scale	Shape	Mean	Standard deviation	Skewness
Length	44.7329	0.2907	1.0720	44.9025	0.2361	0.1591
Diameter	23.9526	0.1830	1.1358	24.0622	0.1466	0.1795

To confirm the conclusions obtained by the previous tests of goodness-of-fit we have used the likelihood ratio test presented in Section 2.2. As we obtained an observed value $-2 \ln \Lambda_{obs} > 3.84$ (for length's and diameter's data), there is a strong evidence that the $SN(\hat{\lambda}, \hat{\delta}, \hat{\alpha})$ distribution presents a better fit than the normal $N(\hat{\mu}, \hat{\sigma}^2)$ distribution, for a level of significance of 5%.

Finally, based on Algorithm 3.1., we illustrate the implementation of the M and S bootstrap control charts for subgroups of size $n = 10$ to monitor the process mean value and the process standard deviation of the corks' diameter. The Phase I data set consists of $m = 25$ subgroups of size $n = 10$, and we were led to the following control limits: $LCL=23.936484$ and $UCL=24.215071$ for the M -chart, and $UCL=0.249708$ for the S -chart. From these subgroups we have also estimated the control limits of the corresponding Shewhart charts, assuming normality, here denoted, LCL_{sh} and UCL_{sh} , and the center line, CL . We obtained $LCL_{sh}=23.947788$, $UCL_{sh}=24.200532$, $LC=24.07416$ for the M -chart, and $UCL_{sh}=0.223152$, $CL=0.129573$ for the S -chart.

In Figure 4 we picture the M and S bootstrap control charts together with the corresponding Shewhart charts with estimated control limits, to be used in Phase II of the process monitoring. We immediately observe that the bootstrap control limits, LCL and UCL, are set up farther apart than the control limits of the Shewhart M and S charts, LCL_{sh} and UCL_{sh} .

The Phase II data set used in this illustration consists of $m = 50$ subgroups of size $n = 10$, supposed to be in-control. We have computed the statistics \bar{x} and s associated to these 50 subgroups, and we have plotted them in the charts (here denoted M and S). While the bootstrap charts do not signal changes in the process parameters, the Shewhart charts indicates that the process is out-of-control, due to changes in the process mean value and standard deviation.

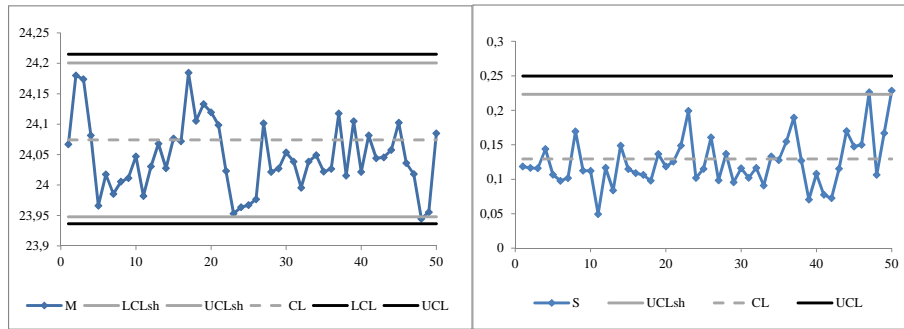


Figure 4: Bootstrap M and S charts together with the corresponding Shewhart charts with estimated control limits.

ACKNOWLEDGMENTS

This work was partially sponsored by National Funds through **FCT**—Fundação para a Ciência e a Tecnologia, project PEst-OE/MAT/UI0006/2011.

REFERENCES

- [1] ABTAHI, A., TOWHIDI, M. AND BEHBOODIAN, J. (2011). An appropriate empirical version of skew-normal density. *Statistical Papers*, **52**, 469-489.
- [2] AZZALINI A. (1985). A Class of distributions which includes the normal Ones. *Scandinavian J. of Statistics*, **12**, 171-178.

- [3] AZZALINI A. (1986). Further results on a class of distributions which includes the normal ones. *Statistica*, **XLVI**, 199-208.
- [4] AZZALINI A. (2005). The skew-normal distribution and related multivariate families. *Scandinavian J. of Statistics*, **32**, 159-188.
- [5] AZZALINI A. (2011). R package 'sn': The skew-normal and skew-t distributions (version 0.4-17). URL <http://azzalini.stat.unipd.it/SN>.
- [6] AZZALINI, A. AND CAPITANIO, A. (1999). Statistical applications of the multivariate skew normal distributions. *J. R. Stat. Soc.*, series B **61**, 579-602.
- [7] BAI, D.S. AND CHOI, I.S. (1995). \bar{X} and R control charts for skewed populations, *J. of Quality Technology*, **27**(2), 120-131.
- [8] EFRON, B. AND TIBSHIRANI, R. (1993). *Introduction to the Bootstrap*, Chapman and Hall, New York.
- [9] FERNANDEZ C. AND STEEL M.F.J. (1998). On Bayesian modeling of fat tails and skewness. *J. Am. Stat. Assoc.*, **93**, 359-371.
- [10] HOAGLIN, D. M., MOSTELLER, F. AND TUKEY, J. W. (1983). *Understanding Robust and Exploratory Data Analysis*, Wiley, New York.
- [11] HOTELLING, H. (1947). Multivariate Quality Control Illustrated by Air Testing of Sample Bombsights. In *Selected Techniques of Statistical Analysis* (C. Eisenhart, M. W. Hastay, and W. A. Wallis, eds.), pp 111-184. McGraw-Hill, New York.
- [12] JAMALIZADEB, A., ARABPOUR, A.R. AND BALAKRISHNAN, N. (2011). A generalized skew two-piece skew normal distribution. *Statistical Papers*, **52**, 431-446.
- [13] JONES, L. A. AND WOODALL, W. H. (1998). The performance of bootstrap control charts. *J. of Quality Technology*, **30**,362375.
- [14] LIO, Y.L. AND PARK, C. (2008). A Bootstrap Control Chart for BirnbaumSaunders Percentiles *Qual. Reliab. Engng. Int.*, **24**, 585-600.
- [15] LIO, Y.L. AND PARK, C. (2010). A bootstrap control chart for inverse Gaussian percentiles *J. of Statistical Computation and Simulation*, **80**(3), 287-299.
- [16] LIU, R. Y. AND TANG, J. (1996). Control charts for dependent and independent measurements based on the bootstrap. *JASA*, **91**, 16941700.
- [17] MONTGOMERY, D. C. (2005). *Introduction to Statistical Quality Control*, Wiley, New York.
- [18] NICHOLS, M. D. AND PADGETT, W. J. (2006). A Bootstrap Control Chart for Weibull Percentiles, *Qual. Reliab. Engng. Int.*, **22**, 141-151.
- [19] O'HAGAN, A. AND LEONARD, T. (1976). Bayes estimation subject to uncertainty about parameter constraints. *Biometrika*, **63**, 201-202.
- [20] OWEN, D. B. (1956). Tables for computing bivariate normal probabilities. *Ann. Math. Statist.*, **27**, 1075-1090.
- [21] SEPPALA, T., MOSKOWITZ, H., PLANTE, R. AND TANG, J. (1996). Statistical process control via the subgroup bootstrap. *J. of Quality Technology*, **27**, 139153.